ADP-15-46/T948

Hamiltonian effective field theory study of the N*(1535) resonance in lattice QCD

Zhan-Wei Liu,[1] Waseem Kamleh,[1] Derek B. Leinweber,[1] Finn M. Stokes,[1] Anthony W. Thomas,[1,2] and Jia-Jun Wu[1]

[1]*Special Research Center for the Subatomic Structure of Matter (CSSM), Department of Physics, University of Adelaide, Adelaide SA 5005, Australia*
[2]*ARC Centre of Excellence in Particle Physics at the Terascale, Department of Physics, University of Adelaide, Adelaide SA 5005, Australia*

Drawing on experimental data for baryon resonances, Hamiltonian effective field theory (HEFT) is used to predict the positions of the finite-volume energy levels to be observed in lattice QCD simulations of the lowest-lying $J^P = 1/2^-$ nucleon excitation. In the initial analysis, the phenomenological parameters of the Hamiltonian model are constrained by experiment and the finite-volume eigenstate energies are a prediction of the model. The agreement between HEFT predictions and lattice QCD results obtained on volumes with spatial lengths of 2 and 3 fm is excellent. These lattice results also admit a more conventional analysis where the low-energy coefficients are constrained by lattice QCD results, enabling a determination of resonance properties from lattice QCD itself. Finally, the role and importance of various components of the Hamiltonian model are examined.

PACS numbers: 14.20.Gk, 12.38.Gc, 13.75.Gx

arXiv:1512.00140v2 [hep-lat] 29 Feb 2016

Lattice QCD has proven remarkably successful in reproducing the masses and many other properties of the octet baryons, which are stable under the strong interaction. In our on-going quest to understand the structure of hadronic systems in terms of QCD, the focus is now shifting to excited states. Perhaps the greatest challenge there is that all states studied on a Euclidean space-time lattice are stable eigenstates of the QCD Hamiltonian, subject to periodic spatial boundary conditions. In contrast, the resonant states revealed in experiments are neither stable, nor are they eigenstates of the QCD Hamiltonian. Rather, they are often extremely short-lived, with multiple decay modes. Clearly one faces an enormous challenge when one aims to use lattice QCD to study these states.

One powerful technique, introduced by Lüscher [1, 2], which has been widely used by the community, does provide a robust link between the discrete energy levels observed in lattice QCD and the scattering phase shifts extracted from experiment. This method presents technical complications when the resonance under study can decay through more than one open channel. These complications can be overcome and the resulting formalism has been successfully applied in the coupled $\pi\pi$ and $K\bar{K}$ system [3]. On the other hand, several groups have been led to explore an alternative approach, which we label Hamiltonian effective field theory (HEFT).

HEFT enables a quantitative examination of experimental observations such as resonance positions, partial decay widths, scattering phase shifts and inelasticities in terms of a model built from hadronic degrees of freedom and their interactions. While formulated in infinite volume, such models have recently been applied to the analysis of the hadronic excitation spectra observed in a small number of finite volume lattice QCD calculations [4, 5], namely the Δ resonance [4] and the $\Lambda(1405)$ [5]. The former is a classical case where a three-quark state is dressed by coupling to the open πN channel, while the latter is far more complex and illustrates some of the power of HEFT. In concert with a lattice study of the individual quark flavor contributions to the magnetic form factor of the baryon, the application of HEFT led to a deeper understanding of the nature of this resonance which has been mysterious for 50 years. That study strongly suggested that the $\Lambda(1405)$ does not have a significant three-quark component in its wave function, rather it is appropriately viewed as a $\bar{K}N$ bound state.

In this Letter we examine the nature of the first negative parity excitation of the nucleon, the $J^P = 1/2^-$ $N^*(1535)$. This state has been the subject of much speculation in the literature [6–9], since it lies above the first positive parity nucleon excited state (the Roper resonance at 1440 MeV), unlike the expectation in the phenomenologically very successful harmonic oscillator model. There have also been suggestions that there may be a significant strange quark component in this resonance, so it could be viewed as a penta-quark. Such questions are central to the modern study of resonances and with its S-wave coupling to both πN and ηN channels this is an ideal case for study using HEFT to analyse modern lattice data. Our study supports the interpretation of the $N^*(1535)$ as primarily a three-quark excitation, with couplings to five-quark components. The states most likely associated with the resonance have a probability of about 50% to contain the bare baryon, at the physical pion mass, in boxes with $L \simeq 2, 3$ fm.

The HEFT used here introduces a bare state, N_0^*, which may be thought of as a three-quark state that would be stable in the absence of coupling to the πN and ηN channels. We do not consider the corrections from $N\pi\pi$ states, which would add significant technical complications, because the branching ratio in the case of the $N(1535)$ is only a few percent [10]. The corresponding Hamiltonian has two parts, a non-interacting or bare Hamiltonian, H_0, and an interacting Hamiltonian, H_I.

In the center-of-mass system, the non-interacting part is

$$H_0 \;=\; |N_0^*\rangle\, m_0\, \langle N_0^*| + \sum_\alpha \int d\vec{k} \; |\alpha(\vec{k})\rangle\, \omega_\alpha(k)\, \langle \alpha(\vec{k})| \,. \quad (1)$$

Here m_0 is the mass of N_0^*, while $|\alpha(\vec{k})\rangle$ denotes either the πN or ηN channel and $\omega_\alpha(k)$ is the corresponding energy, $\omega_\alpha(k) = \sqrt{m_{\alpha_1}^2 + \vec{k}^2} + \sqrt{m_{\alpha_2}^2 + \vec{k}^2}$. Here m_{α_1} and m_{α_2} are masses of the meson and baryon, respectively.

Following Refs. [11–13] where there was an extensive study of scattering data involving nucleon resonances up to 1.8 GeV, the interaction Hamiltonian can be divided into two parts, $H_I = g + v$. Here g describes the interaction between the bare state N_0^* and the multi-particle channels which dress it:

$$g = \sum_\alpha \int d\vec{k} \, \left\{ |\alpha(\vec{k})\rangle\, G_\alpha^\dagger(k)\, \langle N_0^*| + |N_0^*\rangle\, G_\alpha(k)\, \langle \alpha(\vec{k})| \right\} . \quad (2)$$

Here, we take $G_{iN}^2(k) = \frac{3\, g_{N_0^* iN}^2}{4\pi^2\, f^2}\, \omega_i(k)\, u^2(k)$, with $i = \pi$ or η and $\omega_X(k) = \sqrt{k^2 + m_X^2}$. The pion decay constant is $f = 92.4$ MeV and the regulator is taken to be a dipole with mass parameter $\Lambda = 0.8$ GeV. $G_\alpha(k)$ corresponds to the Lagrangian $i\bar{N}_0^* \gamma^\mu \partial_\mu \pi N + h.c.$, in the limit where the baryons are treated non-relativistically and a dipole regulator is used to render the theory finite.

The second part of the interaction Hamiltonian is purely phenomenological. It is taken to be separable, with form factors chosen to reproduce the low energy scattering data, well below the energy region where the resonance dominates. It describes the transitions between meson-baryon state $|\alpha(\vec{k})\rangle$ and meson-baryon state $|\beta(\vec{k'})\rangle$:

$$v = \sum_{\alpha,\beta} \int d\vec{k}\, d\vec{k'} \, |\alpha(\vec{k})\rangle\, V_{\alpha,\beta}^S(k,k')\, \langle \beta(\vec{k'})| \,. \quad (3)$$

For example, the separable form for the interaction in the πN channel is

$$V_{\pi N,\pi N}^S(k,k') = \frac{3\, g_{\pi N}^S\, \tilde{u}(k)\, \tilde{u}(k')}{4\pi^2\, f^2} \,. \quad (4)$$

In order to fit the low energy experimental data well it was found that the form factors needed enhancement at low momentum and the purely ad hoc form $\tilde{u}(k) = u(k)(m_\pi + \omega_\pi(k))/\omega_\pi(k)$, works very well, with $u(k)$ the same function used in Eq. (2). Of course, when exploring the fit to lattice data away from the physical pion mass, the value of m_π appearing in $\tilde{u}$ is *not* varied.

The scattering T matrix is obtained from the relativistic Lippmann-Schwinger equation. The coupling parameters, $g_{N_0^*\pi N}$, $g_{N_0^*\eta N}$, and $g_{\pi N}^S$, and the bare mass m_0 are determined by fitting the empirical phase shifts and inelasticities for πN scattering in the $J = 1/2^-$ channel, with guidance from the partial decay widths of the $N^*(1535)$ resonance. Varying these four parameters and fitting the 56 data points provides the fit illustrated in Fig. 1 with $\chi^2_{\rm dof} = 6.8$ and parameters: $g_{\pi N}^S = -0.0608 \pm 0.0004$, $g_{N_0^*\pi N} = 0.186 \pm 0.006$, $g_{N_0^*\eta N} = 0.185 \pm 0.017$ and $m_0 = 1601 \pm 14$ MeV. This fit yields a pole at $1531 \pm 29 - i\, 88 \pm 2$ MeV on the unphysical energy sheet for πN and ηN, where the error of the pole only counts that of m_0. This is in excellent agreement with the Particle Data Group [10] estimate of $1510 \pm 20 - i\, 85 \pm 40$.

With the Hamiltonian model and associated parameters constrained by experimental data, we can now calculate the $J^P = 1/2^-$ nucleon spectrum in the finite-volume considered in lattice QCD calculations. In a box with length L, the momentum a particle can carry in any one dimension is constrained to integer multiples of the lowest non-trivial momentum $2\pi/L$. In three dimensions, it is convenient to introduce the integer $n = n_x^2 + n_y^2 + n_z^2$ such that the momenta available on the lattice are described by $k_n = 2\pi\sqrt{n}/L$. Full details of the translation of a Hamiltonian of the form given above into a Hamiltonian matrix on a finite spatial volume may be found in Ref. [4].

It has proven extremely useful in unravelling pieces of the strong interaction puzzle to move beyond the physical quark masses to the realm where they become larger. To explore this regime we allow the bare mass, m_0, to vary linearly with quark mass, so that (because $m_\pi^2 \sim m_q$), $m_0(m_\pi^2) = m_0|_{\rm phys} + \alpha_0(m_\pi^2 - m_\pi^2|_{\rm phys})$. In the first instance, α_0 is estimated through a single parameter fit to current lattice QCD results for the $J^P = 1/2^-$ nucleon spectrum. The pion mass dependence of the ground state nucleon mass, $m_N(m_\pi^2)$, is obtained via linear interpolation between the lattice QCD results on the same size lattice. The mass of the η meson is related to the pion mass via $m_\eta^2(m_\pi^2) = m_\eta^2|_{\rm phys} + \frac{1}{3}(m_\pi^2 - m_\pi^2|_{\rm phys})$.

The left-hand plot of Fig. 2 illustrates results from the Hadron Spectrum Collaboration [15, 16] (denoted JLab) and Lang and Verduci [17]. These precise results are obtained on the smaller of the two lattice volumes considered herein, with length $L \simeq 1.98$ fm. The right-hand plot illustrates lattice QCD results for lattice volumes with length $L \approx 2.90$ fm. Recent results from the Centre for the Subatomic Structure of Matter (CSSM) lattice group in Adelaide [18–21] are shown, along with the Cyprus collaboration's results, obtained using the Athens Model Independent Analysis Scheme (AMIAS) [22]. Both groups provide results for light pion masses $\simeq 160$ MeV. The two lowest-lying odd-parity states from lattice QCD have an energy similar to the non-interacting S-wave πN scattering threshold. CSSM reports two more low-lying states typically split by 100 MeV. The Cyprus collaboration reports one state in this regime with an energy consistent with the lower of the two CSSM states.

The precision of the low-lying state observed by Lang and Verduci on the 2 fm lattice highlights the different method employed in their analysis. There the low-lying

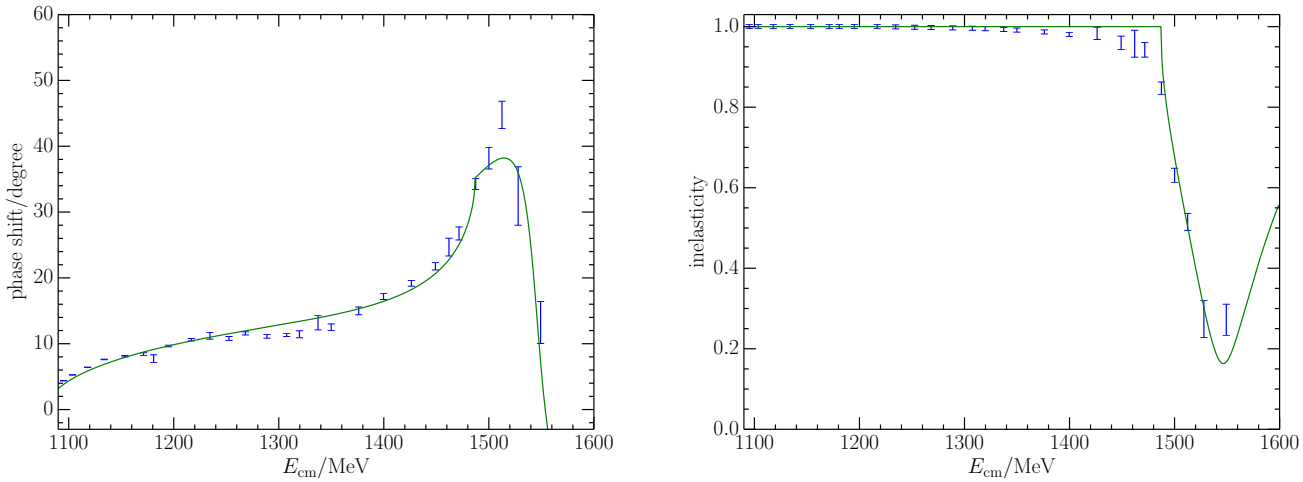

FIG. 1: **Colour online:** Experimental data [14] for the phase shift (left) and inelasticity (right) for πN scattering with $J^P = 1/2^-$ are fit by the Hamiltonian model.

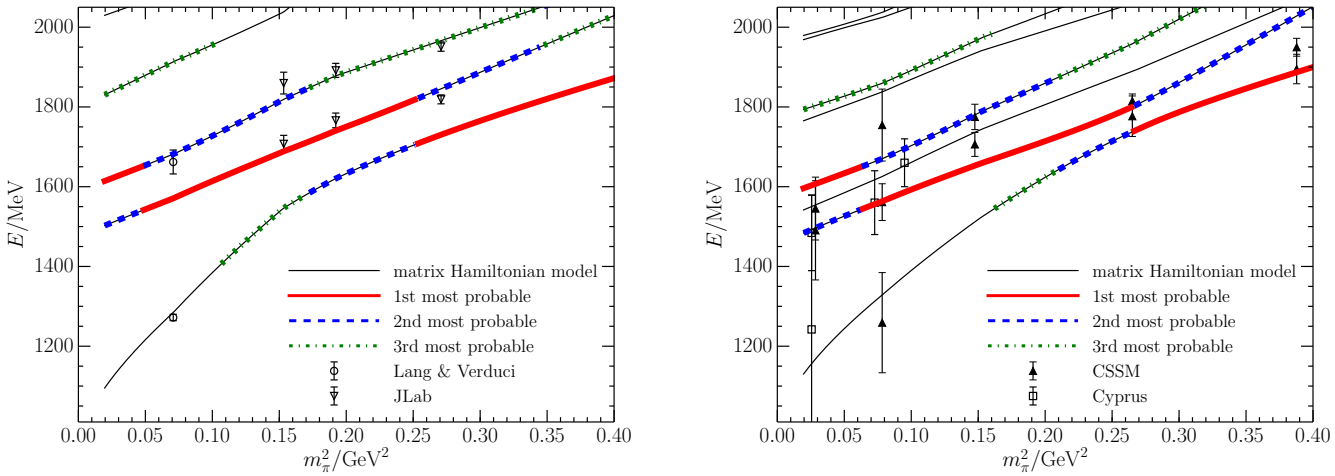

FIG. 2: **Colour online:** The pion mass dependence of the $L \simeq 1.98$ fm (left) and $L \simeq 2.90$ fm (right) finite-volume energy eigenstates. The different line types and colours indicate the strength of the bare basis state in the Hamiltonian-model eigenvector.

scattering state was obtained by creating a meson-baryon source in which the momentum of each hadron is projected to zero. In all other cases, the hadrons have been created using conventional smeared-source operators. To obtain the low-lying state next to the non-interacting S-wave πN scattering threshold, the CSSM collaboration used five-quark operators. All other states have been obtained through the consideration of three-quark operators.

In solving the matrix Hamiltonian the non-interacting basis states mix to form eigenstates of the Hamiltonian. These eigenstate energies are illustrated in Fig. 2 for lattice lengths $L \simeq 1.98$ (left) and 2.90 fm (right). Only one model parameter has been adjusted in fitting 23 lattice energy eigenstates over three levels on two volumes. The parameter $\alpha_0 = 0.96 \pm 0.06$ GeV^{-1}, describing the quark-mass dependence of the bare N^* mass, was obtained from a simultaneous fit of these data providing a $\chi^2_{\rm dof} = 1.7$. Of particular note is the excellent agreement between the high-precision first state reported by Lang and Verduci [17] and the Hamiltonian model.

Because the majority of the states observed in the lattice QCD simulations have their origin in three-quark operators, we examine the eigenvectors of the Hamiltonian states to identify states formed with a large component of the bare basis state. Under the assumption that the three-quark operators couple most strongly to this bare state component, one can then identify states in the matrix Hamiltonian spectrum most likely associated with the states observed in the lattice QCD simulations. In

Fig. 2 we have indicated the strength of the bare-state component through different line types and colours. In both figures, the lattice QCD results expected to be associated with resonant states are indeed described well by the Hamiltonian model. The Hamiltonian states dominated by the bare-state component agree with the lattice results at the one-standard-deviation level.

On comparing the Hamiltonian spectra presented in Fig. 2 one observes a significant dependence on the volume of the lattice considered. The additional complexity of the spectrum encountered on larger lattice volumes is also apparent in the right-hand plot of Fig. 2. Here additional meson-baryon dominated states appear next to the eigenstates seen on the lattice. Future simulations will include new meson-baryon operators to capture these states in the lattice correlation-matrix based variational analyses.

The lowest lying state on both lattice volumes is a πN scattering state at light quark masses, but this evolves into a state dominated by the bare-mass component at heavy quark masses. Here, as the mass of the multi-particle state becomes very large, the lowest-lying state is composed of a bare N^* state dressed by πN and ηN contributions. The third eigenstate on the $L \simeq 2.90$ fm lattice which appears between the two resonant-like lattice states is seen to be predominately an ηN scattering state.

Next we turn to a more traditional analysis, where the aim is to extract information on the resonance of interest. In this case, the low-energy coefficients of the model, the bare mass m_0 and associated slope α_0, are both constrained by the lattice QCD results. After extracting these parameters from the fit to lattice data, we take the infinite volume limit and calculate the pole position. In optimising these parameters, the Hamiltonian eigenstates dominated by bare-state contributions are brought as close as possible to the resonant-like lattice QCD results. Similarly, the first state of the Hamiltonian model is brought as close as possible to the lowest-lying scattering states observed on the lattice. A standard χ^2 measure weighted by the lattice QCD energy uncertainties is used. The resultant fit is very good, with $\chi^2_{\rm dof} = 1.7$. The main change is a slight increase in the bare mass to better accommodate the lattice QCD data at moderate pion masses. Using a bootstrap analysis to determine the standard errors from the percentiles of the distributions, we find $m_0 = 1644\,^{+34}_{-30}$ MeV and $\alpha_0 = 0.77\,^{+0.15}_{-0.16}$ GeV^{-1}, with the position of the pole in the complex plane at: $1602 \pm 48 \, - \, i\,88.6\,^{+0.7}_{-2.8}$ MeV. The pole position lies just outside of a one-sigma agreement with the Particle Data Group estimate of $1510 \pm 20 - i\,85 \pm 40$.

The previous analysis included a background separable interaction which had been constrained by experimental data. Next, we explore the importance of such terms by dropping them and using only the information provided by the lattice calculation. This is necessary, for example, when there is insufficient experimental information on its properties, especially its couplings to hadronic channels. In particular, we fit the lattice QCD results by adjusting the two low-energy coefficients, m_0 and α_0, but this time with the separable potential terms discarded. The optimal fit yields a rather high $\chi^2_{\rm dof} = 4.6$, largely because of the significant discrepancy between the Hamiltonian model prediction for the lowest lying πN scattering state on the $L \simeq 1.98$ fm lattice and the lattice QCD result of Lang and Verduci [17]. The majority of the resonant-like lattice results are still described well by the Hamiltonian model. Using a bootstrap analysis to obtain the uncertainties, the optimal parameters are $m_0 = 1623\,^{+33}_{-41}$ MeV, $\alpha_0 = 0.85\,^{+0.17}_{-0.17}$ GeV^{-1}, Re(pole) $= 1563\,^{+52}_{-80}$ MeV, $-$Im(pole) $= 89.2\,^{+0.2}_{-4.2}$ MeV. This pole position compares favorably with the Particle Data Group's estimate of $1510 \pm 20 - i\,85 \pm 40$. However, the discrepancies highlighted and the associated unacceptable $\chi^2_{\rm dof} = 4.6$ reveals that the separable potential terms are vital to an accurate description of the lattice QCD results.

In summary, we have used Hamiltonian effective field theory (HEFT) to study the low-lying $J^P = 1/2^-$ excitations of the nucleon in both the finite volume of lattice QCD and the infinite volume of nature. We have drawn on experimental data for the lowest-lying $J^P = 1/2^-$ nucleon resonance, the $N^*(1535)$, and used HEFT to predict the positions of the finite-volume energy levels to be observed in lattice QCD simulations in volumes of ~ 2 and ~ 3 fm.

The agreement between the HEFT predictions and lattice QCD results is excellent and admits a more conventional analysis where the low-energy coefficients are constrained by lattice QCD results, enabling a determination of resonance properties from lattice QCD. We used lattice QCD results from two different volumes to determine the pole position of the $N^*(1535)$. We find the pole position $1602 \pm 48 - i\,88.6\,^{+0.7}_{-2.8}$ MeV, which lies just outside of one-sigma agreement with the Particle Data Group estimate of $1510 \pm 20 - i\,85 \pm 40$.

We also examined the role of πN separable potential couplings and found them to be essential in accurately describing the position of the lowest-lying scattering state in the finite volume of the lattice. The lattice length dependence of the spectrum shows a rich structure and it will be interesting to examine this in detail in future lattice QCD calculations.

Finally, the success of this approach leads us to consider its application to other J^P baryon channels. The $1/2^+$ channel of the nucleon is of particular interest where evidence of the Roper resonance in lattice QCD investigations is providing a fascinating puzzle [23] waiting to be solved. Application of the successful formalism presented herein will be of benefit in unravelling the mystery surrounding the Roper resonance in QCD.

Acknowledgments

This research is supported by the Australian Research Council through the ARC Centre of Excellence for Particle Physics at the Terascale, and through Grants DP120104627, DP150103164, DP140103067, LE120100181 (DBL) and FL0992247 and DP151103101 (AWT).

[1] M. Luscher, Commun. Math. Phys. **104**, 177 (1986).
[2] M. Luscher, Commun. Math. Phys. **105**, 153 (1986).
[3] J.-J. Wu, T. S. H. Lee, A. W. Thomas, and R. D. Young, Phys. Rev. **C90**, 055206 (2014), 1402.4868.
[4] J. M. M. Hall, A. C. P. Hsu, D. B. Leinweber, A. W. Thomas, and R. D. Young, Phys. Rev. **D87**, 094510 (2013), 1303.4157.
[5] J. M. M. Hall, W. Kamleh, D. B. Leinweber, B. J. Menadue, B. J. Owen, A. W. Thomas, and R. D. Young, Phys. Rev. Lett. **114**, 132002 (2015), 1411.3402.
[6] J. Nieves and E. Ruiz Arriola, Phys. Rev. D **64**, 116008 (2001).
[7] N. Kaiser, P. Siegel, and W. Weise, Physics Letters B **362**, 23 (1995).
[8] T. Inoue, E. Oset, and M. J. Vicente Vacas, Phys. Rev. C **65**, 035204 (2002).
[9] B. C. Liu and B. S. Zou, Phys. Rev. Lett. **96**, 042002 (2006).
[10] K. A. Olive et al. (Particle Data Group), Chin. Phys. **C38**, 090001 (2014).
[11] H. Kamano, S. X. Nakamura, T.-S. H. Lee, and T. Sato, Phys. Rev. C **88**, 035209 (2013).
[12] A. Matsuyama, T. Sato, and T.-S. Lee, Physics Reports **439**, 193 (2007).
[13] H. Kamano, S. X. Nakamura, T.-S. H. Lee, and T. Sato, Phys. Rev. D **84**, 114019 (2011).
[14] The Institute for Nuclear Studies, http://gwdac.phys.gwu.edu/ (online).
[15] R. G. Edwards, J. J. Dudek, D. G. Richards, and S. J. Wallace, Phys.Rev. **D84**, 074508 (2011), 1104.5152.
[16] R. G. Edwards, N. Mathur, D. G. Richards, and S. J. Wallace (Hadron Spectrum Collaboration), Phys. Rev. D **87**, 054506 (2013).
[17] C. Lang and V. Verduci, Phys.Rev. **D87**, 054502 (2013), 1212.5055.
[18] F. Stokes, W. Kamleh, and D. B. Leinweber, in preparation.
[19] A. L. Kiratidis, W. Kamleh, D. B. Leinweber, and B. J. Owen, Phys. Rev. **D91**, 094509 (2015), 1501.07667.
[20] M. S. Mahbub, W. Kamleh, D. B. Leinweber, P. J. Moran, and A. G. Williams, Phys. Rev. **D87**, 094506 (2013), 1302.2987.
[21] M. S. Mahbub, W. Kamleh, D. B. Leinweber, P. J. Moran, and A. G. Williams, Phys. Rev. **D87**, 011501 (2013), 1209.0240.
[22] C. Alexandrou, T. Leontiou, C. N. Papanicolas, and E. Stiliaris, Phys. Rev. **D91**, 014506 (2015), 1411.6765.
[23] D. Leinweber, W. Kamleh, A. Kiratidis, Z.-W. Liu, S. Mahbub, D. Roberts, F. Stokes, A. W. Thomas, and J. Wu (2015), 1511.09146.